Using Boolean Networks to Model Post-transcriptional Regulation in Gene Regulatory Networks

# Using Boolean Networks to Model Post-Transcriptional Regulation in Gene Regulatory Networks[1]

Gianfranco Politano[a,*], Alessandro Savino[a,b], Alfredo Benso[a], Stefano Di Carlo[a], Hafeez Ur Rehman[a], Alessandro Vasciaveo[a]

[a] *Politecnico di Torino, Control and Comp. Engineering Department, Corso Duca degli Abruzzi 24, 10129, Torino (Italy) E-mail: < firstname > . < lastname >@polito.it, URL: http://www.testgroup.polito.it/index.php/bio-menu-home*
[b] *Consorzio Interuniversitario Nazionale per l'Informatica, Verres (AO), IT*

**Abstract**

Gene Regulatory Networks (GRNs) model some of the mechanisms that regulate gene expression. Among the computational approaches available to model and study GNRs, Boolean Network (BN) emerged as very successful to better understand both the structural and dynamical properties of GRNs. Nevertheless, the most widely used models based on BNs do not include any post-transcriptional regulation mechanism. Since miRNAs have been proved to play an important regulatory role, in this paper we show how the post-transcriptional regulation mechanism mediated by miRNAs has been included in an enhanced BN-based model. We resort to the *miR-7* in two *Drosophila* cell fate determination networks to verify the effectiveness of miRNAs modeling in BNs, by implementing it in our tool for the analysis of Boolean Networks.

*Keywords:* miRNA, Gene Regulatory Networks, post-transcriptional regulation, Boolean Networks, Complex Systems, Network Analysis

## 1. Introduction

The genome of an organism plays a crucial role in regulating several cellular processes. With few exceptions, every cell in an organism contains the same genetic material. This implies that, after sequencing the whole genome of several living organisms [1], and after knowing the functional meaning of thousands of proteins encoded by these genomes [2], one of the principal remaining challenges is to understand the mechanisms that regulate gene expression within the genome [3].

The regulation of gene expression is achieved through genetic regulatory systems organized in networks of interactions between genes, proteins and other cellular components. In order to understand complex genetic regulatory networks, a concerted effort among experiments, modeling, and theory is required. In particular, researchers require automated formal modeling techniques and appropriate analysis tools.

Several computational approaches have been proposed and developed in literature ([4] and further references therein) to model Gene Regulatory Networks (GRNs). They include partial/ordinary differential equations [5, 6], linear models [7], Bayesian networks [8, 9], Boolean networks [10, 11] and Petri nets [12]. They can be divided into two groups: 1) *discrete-state* models and 2) *continuous-state* models. Discrete-state models assign a small number of discrete states to each node of the network, avoiding intermediate expression levels. Regulatory interactions between nodes are described by logical functions. Bayesian networks, Boolean networks, and Petri nets belong to this group. Instead, continuous-state models, assume the state of each node of the network to be a continuous function in time of the expression of the input components. Its evolution is modeled resorting to differential *rate* equations. Partial differential equations, (nonlinear) ordinary differential equations, and linear models belong to this group. Their main limitation consists in the difficulty of properly modeling all biochemical reactions governing the interaction among the nodes of the network.

Boolean Networks (BN), introduced by Kauffman [10], have been proved successful in modeling real regulatory networks (e.g., see [13, 14, 15, 16, 17, 18]). In a BN the state of a biochemical entity, i.e., a gene, is described by a Boolean variable. The transition from one state to another state is computed by means of a Boolean function of the states of other genes in the network. Transitions between states are *deterministic*, which means that, given an initial state, the next state is always the same. Although the approach seems to set a strong simplification compared to reality, BNs enable to study high-level properties of complex networks (e.g., robustness to background noise, behavior under different initial conditions, etc.).

Recent researches suggest that several realistic biological problems may be analyzed resorting to the BN formalism. In this cases, BNs allow for a simulation of a real biological GRN's dynamic behavior (e.g., the Drosophila case),

*Corresponding author

emphasizing the functional relevance of the resulting network topology [19]. Biologist are thus able to characterize the network and evaluate its dynamics, identifying topological elements such as *feedback circuits*, i.e., cascades of regulatory interactions, *negative circuits* that buffer gene effects, and *positive circuits* that may constitute developmental switches enabling alternative developmental pathways [20, 21]. Moreover, it is possible to study properties of the biological GRN by computing and analyzing the *attractors* of the network. An attractor is a single state or a set of states towards which a system tends to converge over time [22, 23].

Most published BN based models focus on high-level gene/gene or gene/protein interactions, neglecting post-transcriptional regulatory activities carried out by small non-coding RNA sequences, such as micro RNA (miRNA).

In this paper we discuss how miRNAs and post-transcriptional regulatory interactions can be modeled resorting to BNs. The proposed BN based post-transcriptional model has been implemented in a software tool able to simulate a BN and to compute the attractors of the network taking into account post-transcriptional activities [24].

We exploited the developed model and the related tool to analyze two real networks related to *Drosophila* taken from [25]. Results obtained from the network analysis have been then compared with experimental results discussed in [25] to show the capability of the proposed model to provide interesting insights related to the modeled biological process.

## 2. Background

Modeling general aspects of GRNs, such as genes' interactions, dates back to the end of 1960s. In [10], Kauffman considered an idealized representation of a typical gene network. The assumption is that genes are equivalent entities, and their interaction forms a directed graph in which each gene receives inputs from a fixed number of selected genes. The set of entities populating the network has been recently extended including gene products (e.g., proteins) by [18]. The state of each regulatory entity, i.e., a gene or a protein, is represented as a Boolean value, either 1, indicating the *presence* of the entity (e.g., a gene is expressed), or 0 indicating its *absence* (e.g., a gene is not expressed).

Given a set of $N$ entities, the *state* of the GRN is represented by a Boolean vector $\hat{\mathbf{X}} = [x_1, \cdots, x_N]$, leading to a state space of $2^N$ states. Each component $x_i$ of $\hat{\mathbf{X}}$ is described using a Boolean function $f_i$ ($x_i = f_i\left(\hat{\mathbf{X}}\right)$).

To make the model computationally acceptable, the f behavior of a BN is usually simulated in a *synchronous* way, i.e., all entities of the network update their state together [13, 26]:

$$\hat{\mathbf{X}}^{\mathbf{t+1}} = \hat{\mathbf{F}}\left(\hat{X}^t\right) \quad (1)$$

where $\hat{\mathbf{X}}^{\mathbf{t+1}}$ is the next GRN state and $\hat{\mathbf{F}}$ is the vector of all functions $f_i$ that map the transition of a single entity from the current state to the next one.

During the simulation of the network dynamics, an initialization state sets all nodes of the network to a known configuration. The network state is then continuously updated by repeatedly evaluating all boolean functions describing the network until a *steady* state or a state *cycle* is reached. The sequence of states traversed by a BN during the simulation of its dynamics forms a *trajectory* of the system, while the final steady state or the final state cycle of the trajectory form a *point* or a *cyclic* attractor, respectively. Each network is associated with a set of point and cyclic attractors, depending on its dynamics on different initialization states. In case of a point attractor, the system's state freezes whenever the network enters the attractor, and it is unable to perform further transitions unless external perturbations are applied. Differently, cyclic attractors show a cyclic behavior of the system. Once a trajectory falls into one of the states belonging the attractor, the system keeps cyclically moving among the attractor's states.

To properly study the network dynamics all possible initialization states should be simulated. The set of initial states leading to an attractor is called *basin* of attraction [27]. Attractor's properties (length of cyclic attractors, basins dimensionality, trajectory lengths, etc.) are commonly studied in order to infer high-level properties of a GRN [18, 27].

Figure 1a gives a simple example of a BN. It contains three entities (e.g., $x_1$, $x_2$, $x_3$) whose next state functions are defined as follows:

$$x_1^{t+1} = \neg x_3^t$$
$$x_2^{t+1} = x_1^t \wedge x_3^t$$
$$x_3^{t+1} = x_2^t$$

Figure 1b shows the state space of this network. Each node represents a possible network state whereas edges represent legal state transitions for the network.

## 3. Models and Methods

### *3.1. Extending the Gene Protein/Product Boolean Network Model*

Functional studies indicate that miRNAs participate in the regulation of almost every investigated cellular process like, for instance, cell metabolism, signal transduction, cell differentiation, cell fates and so on [28, 29, 30]. miRNAs regulate gene expression post-transcriptionally by interfering either with a target mRNA's translation or stability [31]. Moreover, further studies show that they can modulate mRNA-protein interactions, and suppress protein synthesis, although the mechanistic details are still poorly understood.

The interaction between mRNAs and proteins is well modeled by the Gene Protein/Product Boolean Network

Figure 1: Example of a simple boolean network involving three genes ($x_1$, $x_2$ and $x3$) together with the related space state.

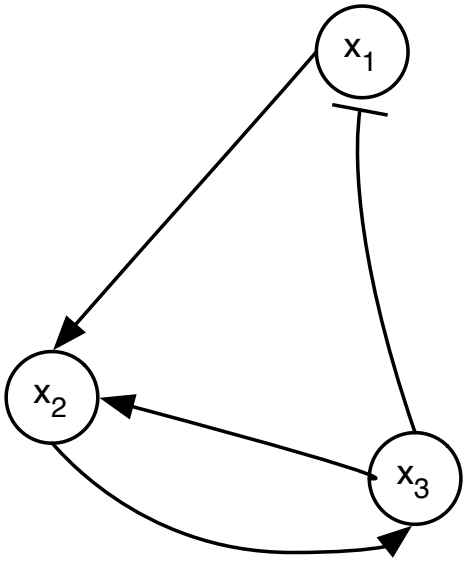


(a) The boolean network represented as a directed graph. Each node of the graph represents a gene while arcs represents gene interactions.

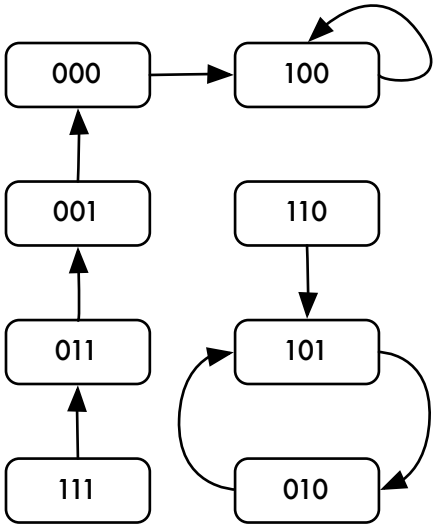


(b) The state space of the network represented as a directed graph where each node represents a state of the network while arcs represent valid state transitions.

(GPBN) model proposed by Graudenzi et al. in [18], which is a generalization of the classical RBN model. In a GPBN, gene to gene interactions are mediated by the synthesis of proteins and other products. However post-transcriptional regulation carried out by miRNAs is still not fully considered. Figure 2 depicts a very simple example of GRN modeling a cellular regulatory activity that includes all entities that need to be considered in order to extend the GPBN model to include post-transcriptional regulation mechanisms. According to the example, G1 and G2 are transcribed into two mRNA molecules (mRNA1 and mRNA2); P1 and P2 are the resulting proteins. P2 works as an upstream promoter of gene G3, i.e., G2 is a transcription factor of gene G3. miRNA1 (still a *product* of G1) acts as a post-transcriptional repressor of mRNA2, which results in a translational repression of P2 and therefore in an inhibition effect on gene G3.

To properly model this post-transcriptional interaction, following the GPBN principles, we extended the interaction between genes (G1 and G2 of the example) by explicitly introducing their related products (as previously done for continuous models [32, 33]), thus, including miRNA1 as a *product* of G1.

Figure 3 shows an extended BN representing the proposed regulatory example. For the sake of simplicity, the translational process that leads to the protein production, starting from the related mRNA molecule, has not been explicitly modeled. Nevertheless, if necessary, the model can be easily extended by adding all actors required to precisely modeling all processes. Networks nodes are depicted with different symbols to identify: (1) *genes* (circular nodes), (2) *mRNA_Protein* pairs (rectangular nodes), and (3) *miRNA* (rhomboidal nodes).

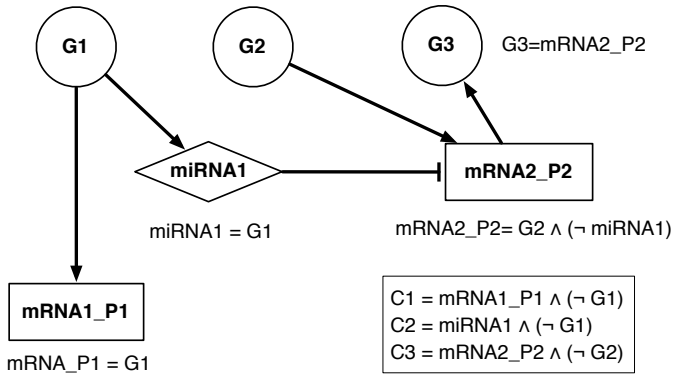


Figure 3: Boolean network model of the GRN proposed in Figure 2 including explicit modeling of post-transcriptional regulatory activity.

In order to properly model the post-transcriptional regulation mechanisms, the set of boolean functions of each transcriptional product targeted by a miRNA (e.g., the *mRNA2_P2* node) must be carefully designed. Post-transcriptional regulation acts at mRNA level, hence, considering the final protein production, it has higher priority compared to gene expression activity. In terms of Boolean

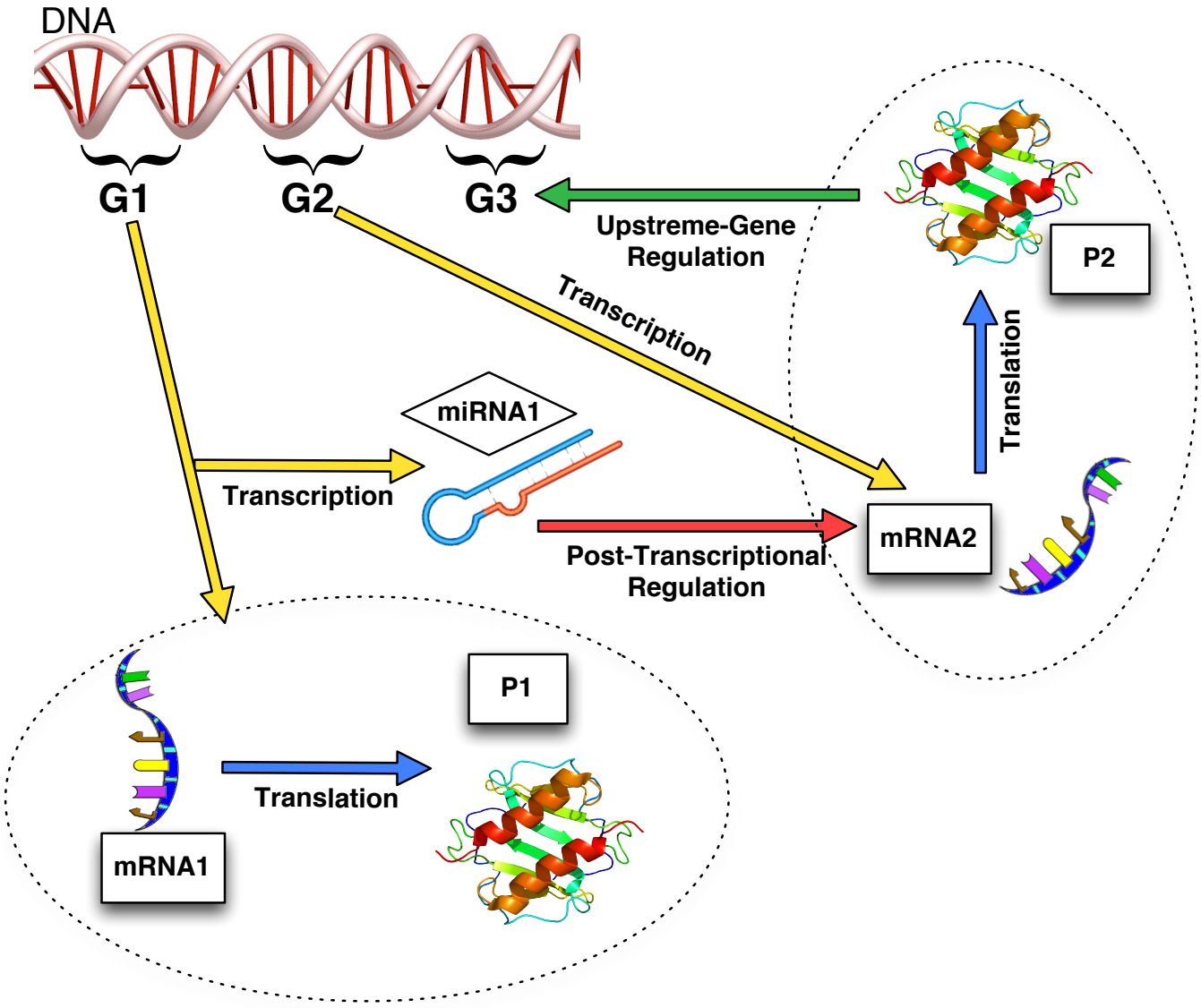


Figure 2: Example of a GRN involving post-transcriptional mechanisms.

functions, this can be modeled by placing the miRNA expression state in Boolean AND with the mRNA expression state.

When introducing gene products such as proteins and miRNAs in a BN model, the synthesis and decay times for a given product must be taken into account. In our model, we considered an unitary synthesis and decay time for all entities according to the GPBN model. Therefore, the change of state of a gene at time $t$ influences all its products at time $t+1$.

Although the introduction of miRNA entities into the BN makes it possible to account for their post-transcriptional activity into the dynamics of the system, it is not enough to properly model the whole post-transcriptional activity. If not properly constrained, users may select initialization states for the simulation of the network (that can now include combinations of genes and products) that may be biologically not valid. To deal with illegal states, the description of the BN is expanded, including a set of conditions identifying all illegal states of the network. Once a biologically valid initialization state is selected, if well designed, the network itself will avoid to evolve into biological illegal states. In Figure 3 these conditions are represented by the Boolean equations C1, C2, and C3. Every time an initial state of the network is considered the three conditions must be evaluated. A state is considered *legal* if all conditions return zero, *illegal* otherwise. As an example, let us consider G1 and the related protein *mRNA1_P1*. The protein can be synthesized only if the related gene has been expressed. So, any state in which *mRNA1_P1* is equal to 1 (expressed), while G1 is equal to 0 (not expressed) is actually an illegal state.

*3.2. Including the model into the Boolean Network Toolkit*

We implemented the GRN model presented in Section 3.1 into a software tool able to analyze the network dynamics by computing the network attractors [24]. The actual implementation is based on the Boolean Network Toolkit (BNT) presented in [26]. The BNT implements the BN direct graph using adjacent lists to optimize access speed and reduce memory allocation. The core is entirely built upon the BOOST C++ Library [34], which provides very efficient and cross platform libraries.

Algorithm 1 shows the overall attractors search process that is an iterative process involving *probes* iterations. *Probes* is the number of initial states from which the network is simulated to identify its attractors. Whenever the number $N$ of network nodes leads to a state space too large to be exhaustively analyzed, it is possible to keep the computation time under control by selecting a reduced set of randomly or user selected initial states for the network. At each iteration, a candidate initial state is selected and its validity against the transcriptional and post-transcriptional constraints is checked. If the state is *legal*, the network dynamic is simulated to search for an attractor on the selected trajectory.

```
Data: the Gene Regulatory Network
Result: a Set which contains the attractors
input : probes the number of initial condition to test
forall the probes do
    σ ← generateRandomState;
    isValid ← isValidBooleanState(σ,C);
    if isValid = true then
        anAttractor ← findAttractor(σ);
        grnAttractorSet.add(anAttractor);
    else
        continue;
```

**Algorithm 1:** GRN attractors searching algorithm.

The isValidBooleanState function (see Algorithm 2) performs the initial state validity check. Given the initial state to analyze and the set of constraints as input, this function evaluates the state against each constraint. If at least one of the constraints is true, it means the given state is not valid and it needs to be discarded. Otherwise, a true value is returned.

Eventually, the tool exports all result of the network analysis (e.g., attractors, state space, trajectories, etc.) using the XGMML format, which is ready to be visualized and further analyzed with visualization tools such as Cytoscape [35].

## 4. Results and Discussion

We tested our model against two real networks discussed in [25]. Both networks analyze the role of *miR-7* in *Drosophila*. The two networks have been modeled resorting to the proposed BN post-transcriptional model and then analyzed by computing the exhaustive set of attractors and trajectories. Results obtained from the network analysis have been finally compared with the results reported in [36] that hypothesize a stabilizing role of *miR-7* against perturbations that would change the cell fate in terms of development. This comparison provides an interesting example of the type of analysis and results that the proposed model is able to support.

```
Result: if the state is admissible or not
input : X the state to check
input : stateConstraintSet the collection of
        constraints for the given network
output: true if the state being checked is admissible
output: false otherwise
notValid ← false;
foreach anInvalidSchema in stateConstraintSet do
    notValid ← isValid OR anInvalidSchema (X) ;
if notValid = true then
    return false ;
else
    return true ;
```

**Algorithm 2:** Algorithm for checking the validity of an initial state.

The simulated networks described using the input formalism of our tool, as well as all outputs produced from the network analysis in standard XGMML format have been provided as additional material to this paper [2] .Moreover the source code of the tool used for the analysis, as well as a legacy Cytoscape plugin that can be used to visualize the outputs produced by the tool can be freely downloaded at `http://www.testgroup.polito.it/index.php/bio-menu-tools/item/208-boolean-regulatory-network-simulator`.

*4.1. Networks description*

The two considered GRNs that regulate the determination of photoreceptor cells, proprioceptor organs, and olfactory organs in *Drosophila* are:

1. *Photoreceptor determination network* (Figure 4a): in this network *miR-7* acts in a coherent feed-forward loop cooperating with *Pnt-P1* in silencing *YAN* to create stability against fluctuations of *Pnt-P1*. This behavior is common for guaranteeing that a cell's fate change is not spontaneously induced or reverted [37], admitting only oriented transitions from the state *YAN* ON to the state *YAN* OFF in which *YAN* itself

[2] We have been unable to submit the supplemental material through the EES submission system. For the review process, this material is therefore available at the following URL: `http://orion.polito.it/tmp/JOCS-D-13-00019-AdditionalMaterial.zip`.

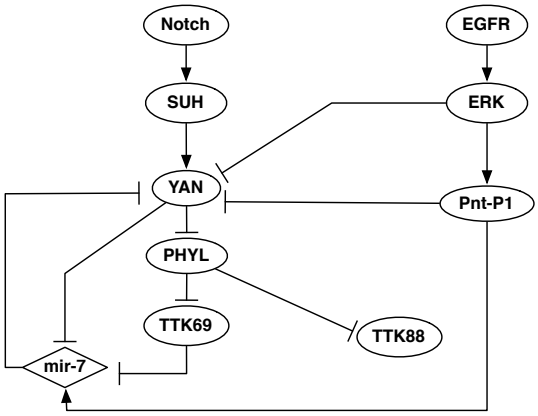


(a) GRN controlling the photoreceptor determination in *Drosophila* as published in [25].

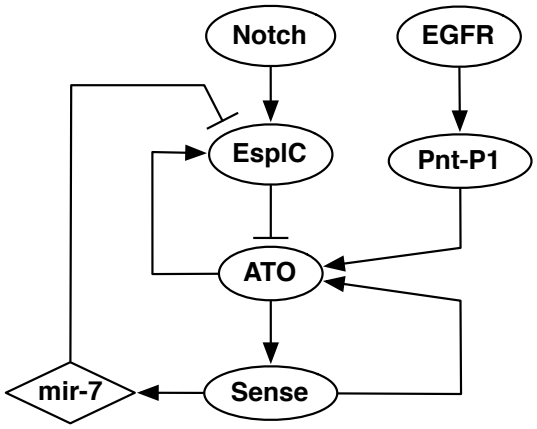


(b) GRN controlling the SOP determination in *Drosophila* as published in [25].

Figure 4: Gene regulatory networks controlling photoreceptor determination and SOP determination in *Drosophila* as published in [25]

is fully degraded. After *YAN* degradation, possible *Pnt-P1* fluctuations will not lead to further *YAN* ON states.

2. *Sensory organ precursor (SOP) determination network* (Figure 4b): in this network *mir-7* belongs to an incoherent feed-forward loop. This type of network motif leads to an accelerated and transient pulse to downstream genes expression [38]. The overall effect is a network in which fluctuating peaks of *Atonal* (*ATO*) would result in transient pulses of *ATO* repression by *EsplC*. Vice versa the sustained increase of *ATO* would result in sustained repression of *EsplC* by *miR-7* and a corresponding stabilization of *ATO* [25].

### *4.2. Network modeling and attractor analysis*

Both networks presented in Figure 4 have been partially redesigned in order to fit our extended GPBN model in which miRNAs target proteins nodes and miRNAs are produced thanks to the expression of the related hosting genes. Figure 5 graphically shows the basic rule exploited during the BN post-transcriptional redesign process. According to [20], if the transcription/translation is active, mRNAs/proteins are synthesized in a one time step. Thus, if the network includes a miRNA node targeting a gene, a new protein node must be inserted in the network. The protein node must be connected to the parent gene node and targeted by the miRNA. Also all gene products (outgoing edges) must be re-arranged accordingly. These extensions respect the assumption that both transcription factors and proteins undergoing post-transcriptional modifications decay in a one time step if their mRNAs are not present [20]. Finally, also the miRNA host gene (if not present) must be explicitly inserted in the network.

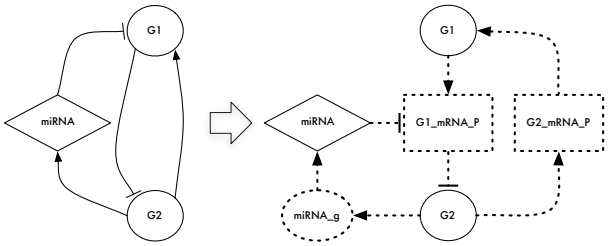


Figure 5: Transformation rules of a traditional boolean network to account for post-transcriptional activities

While this redesign phase has been performed manually on-going work is being carried out to make it automatic within our simulation tool.

Figure 6a and Figure 7a show the redesigned networks considered in our analysis. It is worth to point out here that there is no evidence in [39] regarding the way genes cooperate in enhancing/silencing their products. In order to take into account different options two variants of each network have been considered assuming that:

- a gene is expressed when *all* its parent nodes are concurrently expressed (ON): this condition models enhancer complexes composed by multiple proteins that cooperate together. Resulting boolean functions describe this condition as a set of terms computed by the $\wedge$ operator.

- a gene is expressed when *at least one* of its parent nodes is expressed (ON): this represents the behavior of multiple transcription factors that autonomously induce the expression of their targets. Resulting boolean functions describe this condition as a set of terms computed by the $\vee$ operator.

In both networks, these two options have been modeled by introducing the generic Boolean operator $< op > \in \{\wedge, \vee\}$.

Moreover, in order to highlight the contribution of *miR-7* to the behavior of the network, we compared the two variants of the redesigned networks reported in Figure 6a and Figure 7a, with two equivalent networks in which the

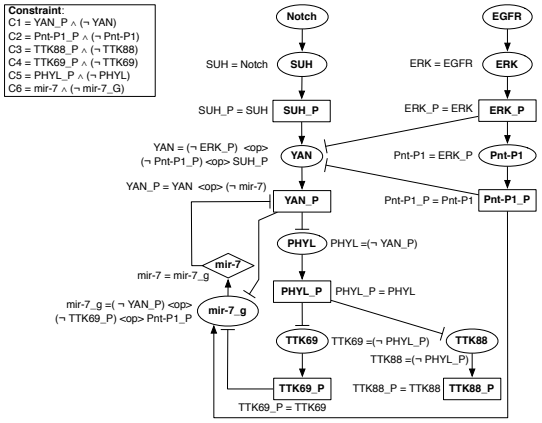


(a) Photoreceptor determination network with *miR-7* present.

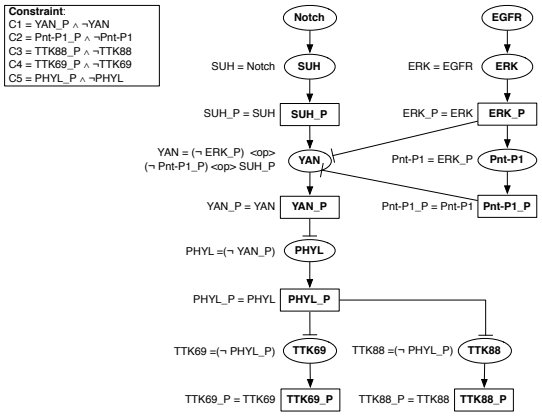


(b) Photoreceptor determination network with *miR-7* absent.

Figure 6: Boolean network modelling the GRN responsible for Photoreceptor Determination in *Drosophila* presented in Figure 4a. The network has been redesigned in order to model post-transcriptional activity considering both the presence and the absence of *miR-7*. The network includes the generic Boolean operator $< op >\in \{\wedge, \vee\}$ that enables to consider different options in the way regulation activity is performed.

*miR-7* node and related edges have been removed (Figure 6b and Figure 7b).

We analyzed each network using our tool, collecting all attractors, trajectories and basins of attraction. Interestingly, the two options introduced by the $< op >$ operator leaded to different behaviors of the network, which still maintains the same topology. In each simulation the exhaustive set of initial states has been analyzed with a reasonable average computation time (˜20-30 msec to analyze each network).

The next sections discuss results obtained from the network analysis. The considered networks have been simulated under several assumptions in order to better understand the properties of the computed attractors, along with the role of *miR-7* in the network.

#### *4.2.1. Photoreceptor determination network*

Due to the network topology, *miR-7* is expected to cooperate with *ERK* and *Pnt-P1* in maintaining the network steady against *YAN* fluctuations.

Given this premise, the comparison of the network attractors between the network with *miR-7* (Figure 6a) and the one without *miR-7* (Figure 6b), does not show any difference when the $< op >= \wedge$ option is selected. The set of common attractors with and without *miR-7* is reported in Table **??**. In fact, the mandatory concurring presence of all silencers of *YAN* somehow masks the role of the miRNA. This is not surprising because, based on their discrete nature, BNs perform a qualitative analysis instead of measuring the gene expression rate from a quantitative perspective. This simplification makes the analysis of complex network feasible, but it possibly masks certain configurations and their intermediate equilibrium. In this scenario, the antagonist roles of *Pnt-P1* and *miR-7* concur in preserving the expected pathway behavior (e.g., the complete degradation of *YAN*), possibly masking the *miR-7* fine tuning effect.

Things change when the network is analyzed under the $< op >= \vee$ option. In this case, the tool returns 3 point attractors common in both the network with *miR-7* (Figure 6a) and the one without *miR-7* (Figure 6b) plus a set of specific attractors. The set of common attractors is reported in Table **??**. These attractors are not discussed here since they do not show any difference between the two considered networks. We identified three point attractors specific of the network with *miR-7* and one point attractor specific of the network without *miR-7*:

- Attractors of the network with *miR-7* (see Table 1): the 3 attractors confirm the expression of *miR-7* and the expected degradation of the *YAN* protein. Interestingly, the three attractors show the suppression of *YAN_P* by the miRNA, with no regards to the expression of the signaling genes (*Notch*, *EGFR*), and the *YAN*'s antagonists (*ERK*, *Pnt-P1*).

- Attractors of the network without *miR-7* (see Table **??**): the point attractor shows no degradation

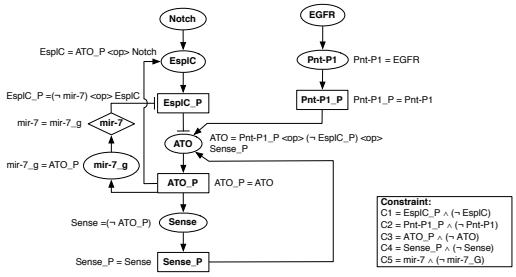


(a) SOP determination network with *miR-7* present.

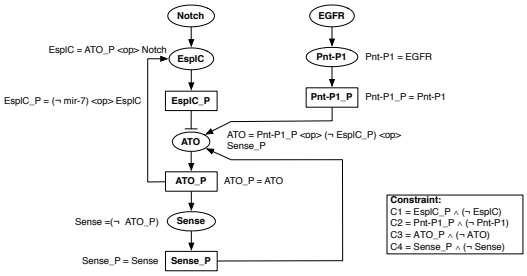


(b) SOP determination network with *miR-7* absent.

Figure 7: Boolean network modeling the GRN responsible for Sensory Organ Precursor (SOP) Determination in *Drosophila* presented in Figure 4b. The network has been redesigned in order to model post-transcriptional activity considering both the presence and the absence of *miR-7*. The network includes the generic Boolean operator $< op > \in \{\wedge, \vee\}$ that enables to consider different options in the way regulation activity is performed.

of the *YAN* protein even if both *YAN*'s antagonists (*ERK*, *Pnt-P1*) are expressed. The ectopic expression of *YAN_P* may confirm the regulatory role of *miR-7* for the network's stabilization.

*4.2.2. SOP determination network*

The topology of the SOP determination network suggests two behaviors: 1) transient pulses of downstream genes expression, 2) specific polarization of upstream genes that leads to the stabilization of the entire network.

Let us first consider the network attractors under the $< op >= \wedge$ assumption. The network with *miR-7* (Figure 7a) and the one without *miR-7* (Figure 7b) manifest a set of five point and four common cyclic attractors (reported in Table **??**). In all of them, *EsplC* and its protein are suppressed, regardless the state of *Notch*. In fact, the suppression of *EsplC* is an obvious outcome because it needs the simultaneous expression of both *Notch* and *ATO* (since they are joined with the $< op >= \wedge$). The *Notch* silencing also leads to a similar result in the set of common cyclic attractors: all of them show transient pulses of *ATO* only when the *Notch* chain is turned OFF.

Moreover, the network with *miR-7* introduces one specific point attractor (see Table **??**). The point attractor leads to the complete degradation of *EsplC_P*, while *EsplC*, *miR-7* and *ATO* are still expressed. Since only the *EsplC* protein is silenced whilst its encoding gene remains expressed, this attractor confirms the regulatory role of the miRNA.

Instead, when considering the $< op >= \vee$ assumption, the network with *miR-7* (Figure 7a) and the one without *miR-7* (Figure 7b) manifest two common point attractors only. They show two outcomes compatible with expectancies in [39]: i) when *Notch* is ON and *EGFR* is OFF, *miR-7* is also OFF, avoiding the silencing of *EsplC_P*; ii) when both *Notch* and *EGFR* are ON, *miR-7* is expressed, correctly degrading *EsplC_P*. The analysis of the basins of common attractors provides additional information to understand these two behaviors: the size of each basin decreases when *miR-7* is introduced within the network, supporting the hypothesis that the presence of the miRNA makes the network less prone to enter in one of the common attractors.

Together with the common attractors (see Table **??**) the network also includes now a set of specific attractors:

- Attractors of the network with *miR-7* (see Table **??**): the set of attractors is composed of three point attractors. All of them show the expected stabilization of the network. The sustained expression of *ATO* and *miR-7* causes the degradation of *EsplC_P*, regardless the fact that *EGFR* and *Notch* are expressed or not.

- Attractors of the network without *miR-7* (see Table **??**): The three point attractors show the same pattern of expression: *ATO*, *ATO_P*, *EsplC*, and *EsplC_P* are always turned ON, regardless of the expression of both *EGFR* and *Notch*. The *ATO* expression seems only regulated by *Sense* because it remains still turned ON even if its signaling chain is turned OFF. Looking at the set of four cyclic attractors, all of them share the degradation of *EGFR* and the expression of *Notch*. This condition leads to the expression of both *EsplC* and *EsplC_P*, unexpected in [39]. The pulses of *ATO* are only driven by the *buffer effect* of *Sense*.

For this network only, it can be easily noticed that the $< op >= \vee$ option produces results that are more coherent with experimental findings reported in the literature.

Overall, given the different attractors obtained with the $< op >= \vee$ and $< op >= \wedge$ operators, this preliminary work highlights how the description of the boolean function of any given node plays a crucial role when dealing with GRNs: a better estimate of the operator should eventually lead to a more reliable set of attractors.

## 5. Conclusions

In this paper we discussed an extended BN model to account for post-transcriptional regulation in GRN simulation. Thanks to this extended model, we discussed the set of attractors of two biologically confirmed networks, focusing on the regulatory role of *miR-7*. Attractors have been compared with networks in which the miRNA was removed. The central role of the miRNA for increasing the

network stability has been highlighted in both the networks, confirming the cooperative stabilizing role of *miR-7*.

The enhanced BN model presented in this paper is only a first step towards a more realistic analysis of the high-level functional and topological characteristics of GRNs. Resorting to the tool facilities, the dynamics of real networks can be analyzed. Thanks to the extended model that includes post-transcriptional regulations, not only the network simulation can be more reliable, but also it can offer new insights on the role of miRNAs from a functional perspective, and this improves the current state-of-the-art, which mostly focuses on high-level gene/gene or gene/protein interactions, neglecting post-transcriptional regulations.

Due to its discrete nature, the BN model may still neglect some regulatory fine adjustments. However, the largest number of the computed attractors, now including miRNAs, still represents meaningful *states* of the network. The simple glimpse into the complexity of the network dynamics, that the toolkit is able to provide, could be used not only as a validation of *in vitro* experiments, but as a real System Biology tool able to rise new questions and drive new experiments.

## Acknowledgement

The authors wish to acknowledge and thank Stefano Benedettini (European Centre for Living Technology, Venice, Italy, e-mail: s.benedettini@unive.it), because its knowledge and support helped us to develop our tool.

[1] T. Werner, Next generation sequencing in functional genomics, Brief Bioinform 11 (5) (2010) 499–511. doi:10.1093/bib/bbq018.

[2] A. Benso, S. Di Carlo, H. urRehman, G. Politano, A. Savino, Using gnome wide data for protein function prediction by exploiting gene ontology relationships, in: Automation Quality and Testing Robotics (AQTR), 2012 IEEE International Conference on, 2012, pp. 497 –502.

[3] K. Kaneko, Life: An introduction to complex systems biology, Vol. 171, Springer Heidelberg, Germany:, 2006.

[4] H. D. Jong, Modeling and simulation of genetic regulatory systems: A literature review, Journal of Computational Biology 9 (2002) 67–103.

[5] A. Csikász-Nagy, D. Battogtokh, K. C. Chen, B. Novák, J. J. Tyson, Analysis of a generic model of eukaryotic cell-cycle regulation, Biophys J 90 (12) (2006) 4361–79. doi:10.1529/biophysj.106.081240.

[6] Y. Fomekong-Nanfack, J. A. Kaandorp, J. Blom, Efficient parameter estimation for spatio-temporal models of pattern formation: case study of drosophila melanogaster, Bioinformatics 23 (24) (2007) 3356–63. doi:10.1093/bioinformatics/btm433.

[7] E. P. van Someren, L. F. Wessels, M. J. Reinders, Linear modeling of genetic networks from experimental data, Proc Int Conf Intell Syst Mol Biol 8 (2000) 355–66.

[8] N. Friedman, M. Linial, I. Nachman, Using bayesian networks to analyze expression data, Journal of Computational Biology 7 (2000) 601–620.

[9] E. J. Moler, D. C. Radisky, I. S. Mian, Integrating naive bayes models and external knowledge to examining copper and iron homeostasis in s. cerevisiae, Physiol Genomics 4 (2) (2000) 127–135.

[10] S. A. Kauffman, Metabolic stability and epigenesis in randomly constructed genetic nets, J Theor Biol 22 (3) (1969) 437–67.

[11] R. Albert, Boolean modelingof genetic regulatory networks, in: E. Ben-Naim, H. Frauenfelder, Z. Toroczkai (Eds.), Complex Networks, Vol. 650 of Lecture Notes in Physics, Springer Berlin Heidelberg, 2004, pp. 459–481.

[12] L. J. Steggles, R. Banks, A. Wipat, Modelling and analysing genetic networks: from boolean networks to petri nets, in: Proceedings of the 2006 international conference on Computational Methods in Systems Biology, CMSB'06, Springer-Verlag, Berlin, Heidelberg, 2006, pp. 127–141.

[13] J. Bower, H. Bolouri, Computational Modeling Genetic & Biochem, Computational Molecular Biology Series, Mit Press, 2001.
URL http://books.google.it/books?id=-9hZDDfMroQC

[14] P. Rämö, J. Kesseli, O. Yli-Harja, Perturbation avalanches and criticality in gene regulatory networks, J Theor Biol 242 (1) (2006) 164–70. doi:10.1016/j.jtbi.2006.02.011.

[15] R. Serra, M. Villani, A. Graudenzi, S. A. Kauffman, Why a simple model of genetic regulatory networks describes the distribution of avalanches in gene expression data, J Theor Biol 246 (3) (2007) 449–60. doi:10.1016/j.jtbi.2007.01.012.

[16] S. Bornholdt, Boolean network models of cellular regulation: prospects and limitations, J R Soc Interface 5 Suppl 1 (2008) S85–94. doi:10.1098/rsif.2008.0132.focus.

[17] B. Wilczynski, E. E. M. Furlong, Challenges for modeling global gene regulatory networks during development: insights from drosophila, Dev Biol 340 (2) (2010) 161–9. doi:10.1016/j.ydbio.2009.10.032.

[18] A. Graudenzi, R. Serra, M. Villani, C. Damiani, A. Colacci, S. A. Kauffman, Dynamical properties of a boolean model of gene regulatory network with memory, J Comput Biol 18 (10) (2011) 1291–303. doi:10.1089/cmb.2010.0069.

[19] R. Thomas, R. D'Ari, Biological feedback, CRC Press, 1990.

[20] R. Albert, H. G. Othmer, The topology of the regulatory interactions predicts the expression pattern of the segment polarity genes in Drosophila Melanogaster, Journal of Theoretical Biology 223 (2003) 1–18.

[21] L. Sánchez, D. Thieffry, A logical analysis of the drosophila gap-gene system, J Theor Biol 211 (2) (2001) 115–41. doi:10.1006/jtbi.2001.2335.

[22] S. Huang, I. Ernberg, S. Kauffman, Cancer attractors: a systems view of tumors from a gene network dynamics and developmental perspective., Seminars in cell & developmental biology 20 (7) (2009) 869–876. doi:10.1016/j.semcdb.2009.07.003.
URL http://dx.doi.org/10.1016/j.semcdb.2009.07.003

[23] J. X. Luo, M. S. Turner, Evolving sensitivity balances boolean networks, PLoS One 7 (5) (2012) e36010. doi:10.1371/journal.pone.0036010.

[24] A. Benso, S. Di Carlo, H. urRehman, G. Politano, A. Savino, Accounting for post-transcriptional regulation in boolean networks based regulatory models, in: IWBBIO 2013, International Work-Conference on Bioinformatics and Biomedical Engineering, 2013, pp. 397–404.

[25] S. Artavanis-Tsakonas, M. D. Rand, R. J. Lake, Notch signaling: cell fate control and signal integration in development, Science 284 (5415) (1999) 770–6.

[26] S. Benedettini, M. Villani, A. Roli, R. Serra, M. Manfroni, A. Gagliardi, C. Pinciroli, M. Birattari, Dynamical regimes and learning properties of evolved boolean networks, Neurocomputing 99 (0) (2013) 111 – 123. doi:10.1016/j.neucom.2012.05.023.
URL http://www.sciencedirect.com/science/article/pii/S0925231212004870

[27] M. Aldana, S. Coppersmith, L. Kadanoff, Boolean dynamics with random couplings, in: E. Kaplan, J. Marsden, K. Sreenivasan (Eds.), Perspectives and Problems in Nolinear Science, Springer New York, 2003, pp. 23–89. doi:10.1007/978-0-387-21789-5_2.
URL http://dx.doi.org/10.1007/978-0-387-21789-5_2

[28] D. G. Hendrickson, D. J. Hogan, H. L. McCullough, J. W. Myers, D. Herschlag, J. E. Ferrell, P. O. Brown, , PLoS Biol 7 (11) (2009) e1000238. doi:10.1371/journal.pbio.1000238.
URL http://dx.doi.org/10.1371%2Fjournal.pbio.1000238

[29] N. Cloonan, M. K. Brown, A. L. Steptoe, S. Wani, W. L. Chan, A. R. R. Forrest, G. Kolle, B. Gabrielli, S. M. Grimmond, The mir-17-5p microrna is a key regulator of the g1/s phase cell cycle transition., Genome Biol 9 (8) (2008) R127. doi:10.1186/gb-2008-9-8-r127.

[30] A. Benso, S. Di Carlo, G. Politano, A. Savino, A new mirna motif protects pathways' expression in gene regulatory networks, in: IWBBIO 2013, International Work-Conference on Bioinformatics and Biomedical Engineering, 2013, pp. 377–384.

[31] H. Hwang, T. J. H. University, Dynamic Regulation of MicroRNAs by Post-transcriptional Mechanisms, Johns Hopkins University, 2009.
URL `http://books.google.it/books?id=BWvTZ6\_NU0YC`

[32] L. Glass, S. A. Kauffman, Co-operative components, spatial localization and oscillatory cellular dynamics, J Theor Biol 34 (2) (1972) 219–37.

[33] L. Glass, S. A. Kauffman, The logical analysis of continuous, non-linear biochemical control networks, Journal of Theoretical Biology 39 (1973) 103–129. doi:10.1016/0022-5193(73)90208-7.

[34] B. Dawes, D. Abrahams, R. Rivera, Boost c++ libraries, [Available Online]: http://www.boost.org/doc/libs/.

[35] Cytoscape, Cytoscape: An open source platform for complex network analysis and visualization, [Available Online]: http://www.cytoscape.org.

[36] E. Hornstein, N. Shomron, Canalization of development by microrna, Nat Genet 38 Suppl (2006) S20–4. doi:10.1038/ng1803.

[37] G. J. Melen, S. Levy, N. Barkai, B.-Z. Shilo, Threshold responses to morphogen gradients by zero-order ultrasensitivity, Mol Syst Biol 1 (2005) 2005.0028. doi:10.1038/msb4100036.

[38] S. Mangan, A. Zaslaver, U. Alon, The coherent feedforward loop serves as a sign-sensitive delay element in transcription networks, J Mol Biol 334 (2) (2003) 197–204.

[39] X. Li, J. J. Cassidy, C. A. Reinke, S. Fischboeck, R. W. Carthew, A microrna imparts robustness against environmental fluctuation during development, Cell 137 (2) (2009) 273–82. doi:10.1016/j.cell.2009.01.058.

| | | | | | | | | | | | | | | | |
|---|---|---|---|---|---|---|---|---|---|---|---|---|---|---|---|
| A1 | **mir-7_G** | **mir-7** | *YAN_P* | **YAN** | *TTK88_P* | *TTK88* | *TTK69_P* | *TTK69* | *SUH* | *Pnt-P1_P* | *Pnt-P1* | **PHYL_P** | **PHYL** | *Notch* | *ERK* | *EGFR* |
| A2 | **mir-7_G** | **mir-7** | *YAN_P* | **YAN** | *TTK88_P* | *TTK88* | *TTK69_P* | *TTK69* | **SUH** | *Pnt-P1_P* | *Pnt-P1* | **PHYL_P** | **PHYL** | **Notch** | *ERK* | *EGFR* |
| A3 | **mir-7_G** | **mir-7** | *YAN_P* | **YAN** | *TTK88_P* | *TTK88* | *TTK69_P* | *TTK69* | **SUH** | **Pnt-P1_P** | **Pnt-P1** | **PHYL_P** | **PHYL** | **Notch** | **ERK** | **EGFR** |

Table 1: Unique attractors for Photoreceptor Determination Network using the operator $< op >= \wedge$ with *miR-7*. The Table shows 3 point attractors. Bold/Green labels indicate ON nodes, whereas Italic/Red labels indicate OFF nodes.

| | | | | | | | | | | | | | |
|---|---|---|---|---|---|---|---|---|---|---|---|---|---|
| A1 | **YAN_P** | **YAN** | **TTK88_P** | **TTK88** | **TTK69_P** | **TTK69** | **SUH** | **Pnt-P1_P** | **Pnt-P1** | *PHYL_P* | *PHYL* | **Notch** | **ERK** | **EGFR** |

Table 2: Unique attractors for Photoreceptor Determination Network using the operator $< op >= \wedge$ without *miR-7*. The Table shows 1 point attractor. Bold/Green labels indicate ON nodes, whereas Italic/Red labels indicate OFF nodes.



| | | | | | | | | | | | | | | |
|---|---|---|---|---|---|---|---|---|---|---|---|---|---|---|
| A1 | *YAN_P* | *YAN* | *TTK88_P* | *TTK88* | *TTK69_P* | *TTK69* | *SUH* | *Pnt-P1_P* | *Pnt-P1* | **PHYL_P** | **PHYL** | *Notch* | *ERK* | *EGFR* |
| A2 | **YAN_P** | **YAN** | **TTK88_P** | **TTK88** | **TTK69_P** | **TTK69** | **SUH** | *Pnt-P1_P* | *Pnt-P1* | *PHYL_P* | *PHYL* | **Notch** | *ERK* | *EGFR* |
| A3 | *YAN_P* | *YAN* | *TTK88_P* | *TTK88* | *TTK69_P* | *TTK69* | *SUH* | **Pnt-P1_P** | **Pnt-P1** | **PHYL_P** | **PHYL** | *Notch* | **ERK** | **EGFR** |
| A4 | *YAN_P* | *YAN* | *TTK88_P* | *TTK88* | *TTK69_P* | *TTK69* | **SUH** | **Pnt-P1_P** | **Pnt-P1** | **PHYL_P** | **PHYL** | **Notch** | **ERK** | **EGFR** |

Table 3: Common attractors for Photoreceptor Determination Network using the operator $< op >= \wedge$. The Table shows 4 point attractors. Bold/Green labels indicate ON nodes, whereas Italic/Red labels indicate OFF nodes.

| | | | | | | | | | | | | | | |
|---|---|---|---|---|---|---|---|---|---|---|---|---|---|---|
| A1 | **YAN_P** | **YAN** | **TTK88_P** | **TTK88** | **TTK69_P** | **TTK69** | *SUH* | *Pnt-P1_P* | *Pnt-P1* | *PHYL_P* | *PHYL* | *Notch* | *ERK* | *EGFR* |
| A2 | **YAN_P** | **YAN** | **TTK88_P** | **TTK88** | **TTK69_P** | **TTK69** | **SUH** | *Pnt-P1_P* | *Pnt-P1* | *PHYL_P* | *PHYL* | **Notch** | *ERK* | *EGFR* |
| A3 | *YAN_P* | *YAN* | *TTK88_P* | *TTK88* | *TTK69_P* | *TTK69* | *SUH* | **Pnt-P1_P** | **Pnt-P1** | **PHYL_P** | **PHYL** | *Notch* | **ERK** | **EGFR** |

Table 4: Common attractors for Photoreceptor Determination Network using the operator $< op >= \vee$. The Table shows 3 point attractors. Bold/Green labels indicate ON nodes, whereas Italic/Red labels indicate OFF nodes.

## Additional files

- **PhD_w_mirna_AND_results.zip**: Photoreceptor determination network with $miR\text{-}7$ present and $< op >= \wedge$ option analysis and simulation results.
- **PhD_w_mirna_AND.net**: Photoreceptor determination network with $miR\text{-}7$ present and $< op >= \wedge$ option description file.
- **PhD_w_mirna_OR_results.zip**: Photoreceptor determination network with $miR\text{-}7$ present and $< op >= \vee$ option analysis and simulation results.
- **PhD_w_mirna_OR.net**: Photoreceptor determination network with $miR\text{-}7$ present and $< op >= \vee$ option description file.
- **PhD_w_mirna.constraints**: Photoreceptor determination network with $miR\text{-}7$ present constraint file to be used both for simulation with $< op >= \wedge$ and $< op >= \vee$ options.
- **PhD_wo_mirna_AND_results.zip**: Photoreceptor determination network without $miR\text{-}7$ present and $< op >= \wedge$ option analysis and simulation results.
- **PhD_wo_mirna_AND.net**: Photoreceptor determination network without $miR\text{-}7$ present and $< op >= \wedge$ option description file.
- **PhD_wo_mirna_OR_results.zip**: Photoreceptor determination network without $miR\text{-}7$ present and $< op >= \vee$ option analysis and simulation results.
- **PhD_wo_mirna_OR.net**: Photoreceptor determination network without $miR\text{-}7$ present and $< op >= \vee$ option description file.
- **PhD_wo_mirna.constraints**: Photoreceptor determination network without $miR\text{-}7$ present constraint file to be used both for simulation with $< op >= \wedge$ and $< op >= \vee$ options.
- **SOP_w_mirna_AND_results.zip**: SOP determination network with $miR\text{-}7$ present and $< op >= \wedge$ option analysis and simulation results.
- **SOP_w_mirna_AND.net**: SOP determination network with $miR\text{-}7$ present and $< op >= \wedge$ option description file.
- **SOP_w_mirna_OR_results.zip**: SOP determination network with $miR\text{-}7$ present and $< op >= \vee$ option analysis and simulation results.
- **SOP_w_mirna_OR.net**: SOP determination network with $miR\text{-}7$ present and $< op >= \vee$ option description file.
- **SOP_w_mirna.constraints**: SOP determination network with $miR\text{-}7$ present constraint file to be used both for simulation with $< op >= \wedge$ and $< op >= \vee$ options.
- **SOP_wo_mirna_AND_results.zip**: SOP determination network without $miR\text{-}7$ present and $< op >= \wedge$ option analysis and simulation results.
- **SOP_wo_mirna_AND.net**: SOP determination network without $miR\text{-}7$ present and $< op >= \wedge$ option description file.
- **SOP_wo_mirna_OR_results.zip**: SOP determination network without $miR\text{-}7$ present and $< op >= \vee$ option analysis and simulation results.
- **SOP_wo_mirna_OR.net**: SOP determination network without $miR\text{-}7$ present and $< op >= \vee$ option description file.
- **SOP_wo_mirna.constraints**: SOP determination network without $miR\text{-}7$ present constraint file to be used both for simulation with $< op >= \wedge$ and $< op >= \vee$ options.

| | | | | | | | | | | | | |
|---|---|---|---|---|---|---|---|---|---|---|---|---|
| A1 | **mir-7_G** | **mir-7** | **Sense_P** | **Sense** | **Pnt-P1_P** | **Pnt-P1** | **Notch** | *EsplC_P* | **EsplC** | **EGFR** | **ATO_P** | **ATO** |

Table 5: Unique attractors for SOP Determination Network using the operator $< op >= \wedge$ with *miR-7*. The Table shows 1 point attractor. Bold/Green labels indicate ON nodes, whereas Italic/Red labels indicate OFF nodes.

| | | | | | | | | | | |
|---|---|---|---|---|---|---|---|---|---|---|
| A1 | *Sense_P* | *Sense* | *Pnt-P1_P* | *Pnt-P1* | *Notch* | *EsplC_P* | *EsplC* | *EGFR* | *ATO_P* | *ATO* |
| A2 | *Sense_P* | *Sense* | *Pnt-P1_P* | *Pnt-P1* | **Notch** | *EsplC_P* | *EsplC* | *EGFR* | *ATO_P* | *ATO* |
| A3 | *Sense_P* | *Sense* | **Pnt-P1_P** | **Pnt-P1** | *Notch* | *EsplC_P* | *EsplC* | **EGFR** | *ATO_P* | *ATO* |
| A4 | **Sense_P** | **Sense** | **Pnt-P1_P** | **Pnt-P1** | *Notch* | *EsplC_P* | *EsplC* | **EGFR** | **ATO_P** | **ATO** |
| A5 | *Sense_P* | *Sense* | **Pnt-P1_P** | **Pnt-P1** | **Notch** | *EsplC_P* | *EsplC* | **EGFR** | *ATO_P* | *ATO* |
| A6 | *Sense_P* | **Sense** | **Pnt-P1_P** | **Pnt-P1** | *Notch* | *EsplC_P* | *EsplC* | **EGFR** | *ATO_P* | **ATO** |
| | **Sense_P** | *Sense* | **Pnt-P1_P** | **Pnt-P1** | *Notch* | *EsplC_P* | *EsplC* | **EGFR** | **ATO_P** | *ATO* |
| A7 | *Sense_P* | **Sense** | **Pnt-P1_P** | **Pnt-P1** | *Notch* | *EsplC_P* | *EsplC* | **EGFR** | *ATO_P* | *ATO* |
| | **Sense_P** | *Sense* | **Pnt-P1_P** | **Pnt-P1** | *Notch* | *EsplC_P* | *EsplC* | **EGFR** | *ATO_P* | *ATO* |
| | *Sense_P* | *Sense* | **Pnt-P1_P** | **Pnt-P1** | *Notch* | *EsplC_P* | *EsplC* | **EGFR** | *ATO_P* | **ATO** |
| | *Sense_P* | *Sense* | **Pnt-P1_P** | **Pnt-P1** | *Notch* | *EsplC_P* | *EsplC* | **EGFR** | **ATO_P** | *ATO* |
| A8 | **Sense_P** | **Sense** | **Pnt-P1_P** | **Pnt-P1** | *Notch* | *EsplC_P* | *EsplC* | **EGFR** | *ATO_P* | *ATO* |
| | **Sense_P** | *Sense* | **Pnt-P1_P** | **Pnt-P1** | *Notch* | *EsplC_P* | *EsplC* | **EGFR** | *ATO_P* | **ATO** |
| | *Sense_P* | *Sense* | **Pnt-P1_P** | **Pnt-P1** | *Notch* | *EsplC_P* | *EsplC* | **EGFR** | **ATO_P** | **ATO** |
| | *Sense_P* | **Sense** | **Pnt-P1_P** | **Pnt-P1** | *Notch* | *EsplC_P* | *EsplC* | **EGFR** | **ATO_P** | *ATO* |
| A9 | **Sense_P** | **Sense** | **Pnt-P1_P** | **Pnt-P1** | *Notch* | *EsplC_P* | *EsplC* | **EGFR** | *ATO_P* | **ATO** |
| | **Sense_P** | *Sense* | **Pnt-P1_P** | **Pnt-P1** | *Notch* | *EsplC_P* | *EsplC* | **EGFR** | **ATO_P** | **ATO** |
| | *Sense_P* | **Sense** | **Pnt-P1_P** | **Pnt-P1** | *Notch* | *EsplC_P* | *EsplC* | **EGFR** | **ATO_P** | **ATO** |
| | **Sense_P** | **Sense** | **Pnt-P1_P** | **Pnt-P1** | *Notch* | *EsplC_P* | *EsplC* | **EGFR** | **ATO_P** | *ATO* |

Table 6: Common attractors for SOP Determination Network using the operator $< op >= \wedge$. The Table shows 5 point attractors and 4 cyclic attractors. Bold/Green labels indicate ON nodes, whereas Italic/Red labels indicate OFF nodes.

| | | | | | | | | | | | | |
|---|---|---|---|---|---|---|---|---|---|---|---|---|
| A1 | **mir-7_G** | **mir-7** | **Sense_P** | **Sense** | *Pnt-P1_P* | *Pnt-P1* | *Notch* | *EsplC_P* | **EsplC** | *EGFR* | **ATO_P** | **ATO** |
| A2 | **mir-7_G** | **mir-7** | **Sense_P** | **Sense** | *Pnt-P1_P* | *Pnt-P1* | **Notch** | *EsplC_P* | **EsplC** | *EGFR* | **ATO_P** | **ATO** |
| A3 | **mir-7_G** | **mir-7** | **Sense_P** | **Sense** | **Pnt-P1_P** | **Pnt-P1** | *Notch* | *EsplC_P* | **EsplC** | **EGFR** | **ATO_P** | **ATO** |

Table 7: Unique attractors for SOP Determination Network using the operator $< op >= \vee$ with *miR-7*. The Table shows 3 point attractors. Bold/Green labels indicate ON nodes, whereas Italic/Red labels indicate OFF nodes.

| | | | | | | | | | | |
|---|---|---|---|---|---|---|---|---|---|---|
| A1 | **Sense_P** | **Sense** | *Pnt-P1_P* | *Pnt-P1* | *Notch* | **EsplC_P** | **EsplC** | *EGFR* | **ATO_P** | **ATO** |
| A2 | **Sense_P** | **Sense** | *Pnt-P1_P* | *Pnt-P1* | **Notch** | **EsplC_P** | **EsplC** | *EGFR* | **ATO_P** | **ATO** |
| A3 | **Sense_P** | **Sense** | **Pnt-P1_P** | **Pnt-P1** | **Notch** | **EsplC_P** | **EsplC** | **EGFR** | **ATO_P** | **ATO** |
| A4 | *Sense_P* | **Sense** | *Pnt-P1_P* | *Pnt-P1* | **Notch** | **EsplC_P** | **EsplC** | *EGFR* | *ATO_P* | **ATO** |
| | **Sense_P** | *Sense* | *Pnt-P1_P* | *Pnt-P1* | **Notch** | **EsplC_P** | **EsplC** | *EGFR* | **ATO_P** | *ATO* |
| A5 | *Sense_P* | *Sense* | *Pnt-P1_P* | *Pnt-P1* | **Notch** | **EsplC_P** | **EsplC** | *EGFR* | *ATO_P* | **ATO** |
| | *Sense_P* | *Sense* | *Pnt-P1_P* | *Pnt-P1* | **Notch** | **EsplC_P** | **EsplC** | *EGFR* | **ATO_P** | *ATO* |
| | *Sense_P* | **Sense** | *Pnt-P1_P* | *Pnt-P1* | **Notch** | **EsplC_P** | **EsplC** | *EGFR* | *ATO_P* | *ATO* |
| | **Sense_P** | *Sense* | *Pnt-P1_P* | *Pnt-P1* | **Notch** | **EsplC_P** | **EsplC** | *EGFR* | *ATO_P* | *ATO* |
| A6 | *Sense_P* | *Sense* | *Pnt-P1_P* | *Pnt-P1* | **Notch** | **EsplC_P** | **EsplC** | *EGFR* | **ATO_P** | **ATO** |
| | *Sense_P* | **Sense** | *Pnt-P1_P* | *Pnt-P1* | **Notch** | **EsplC_P** | **EsplC** | *EGFR* | **ATO_P** | *ATO* |
| | **Sense_P** | **Sense** | *Pnt-P1_P* | *Pnt-P1* | **Notch** | **EsplC_P** | **EsplC** | *EGFR* | *ATO_P* | *ATO* |
| | **Sense_P** | *Sense* | *Pnt-P1_P* | *Pnt-P1* | **Notch** | **EsplC_P** | **EsplC** | *EGFR* | *ATO_P* | **ATO** |
| A7 | *Sense_P* | **Sense** | *Pnt-P1_P* | *Pnt-P1* | **Notch** | **EsplC_P** | **EsplC** | *EGFR* | **ATO_P** | **ATO** |
| | **Sense_P** | **Sense** | *Pnt-P1_P* | *Pnt-P1* | **Notch** | **EsplC_P** | **EsplC** | *EGFR* | **ATO_P** | *ATO* |
| | **Sense_P** | **Sense** | *Pnt-P1_P* | *Pnt-P1* | **Notch** | **EsplC_P** | **EsplC** | *EGFR* | *ATO_P* | **ATO** |
| | **Sense_P** | *Sense* | *Pnt-P1_P* | *Pnt-P1* | **Notch** | **EsplC_P** | **EsplC** | *EGFR* | **ATO_P** | **ATO** |

Table 8: Unique attractors for SOP Determination Network using the operator $< op >= \vee$ without *miR-7*. The Table shows 3 point attractors and 4 cyclic attractors. Bold/Green labels indicate ON nodes, whereas Italic/Red labels indicate OFF nodes.

| | | | | | | | | | | |
|---|---|---|---|---|---|---|---|---|---|---|
| A1 | *Sense_P* | *Sense* | *Pnt-P1_P* | *Pnt-P1* | **Notch** | **EsplC_P** | **EsplC** | *EGFR* | *ATO_P* | *ATO* |
| A2 | **Sense_P** | **Sense** | **Pnt-P1_P** | **Pnt-P1** | **Notch** | *EsplC_P* | **EsplC** | **EGFR** | **ATO_P** | **ATO** |

Table 9: Common attractors for SOP Determination Network using the operator $< op >= \vee$. The Table shows 2 point attractors. Bold/Green labels indicate ON nodes, whereas Italic/Red labels indicate OFF nodes.